Depolymerization

Selective Lanthanide-Organic Catalyzed Depolymerization of Nylon-6 to ε-Caprolactam

Lukas Wursthorn, Kristen Beckett, Jacob O. Rothbaum, Robin M. Cywar, Clarissa Lincoln, Yosi Kratish,* and Tobin J. Marks*

Abstract: Nylon-6 is selectively depolymerized to the parent monomer ε-caprolactam by the readily accessible and commercially available lanthanide trisamido catalysts $Ln(N(TMS)_2)_3$ ($Ln =$ lanthanide). The depolymerization process is solvent-free, near quantitative, highly selective, and operates at the lowest Nylon-6 to ε-caprolactam depolymerization temperature reported to date. The catalytic activity of the different lanthanide trisamides scales with the Ln^{3+} ionic radius, and this process is effective with post-consumer Nylon-6 as well as with Nylon-6+polyethylene, polypropylene or polyethylene terephthalate mixtures. Experimental kinetic data and theoretical (DFT) mechanistic analyses suggest initial deprotonation of a Nylon terminal amido N–H bond, which covalently binds the catalyst to the polymer, followed by a chain-end back-biting process in which ε-caprolactam units are sequentially extruded from the chain end.

Introduction

Our modern society is heavily dependent on plastics-based materials, as evident by the steady growth in their production. In 2002, 200 MT of plastics were produced annually worldwide; in 2018, this output doubled (395 MT), and by 2050 it is expected to triple (≈ 1.2 BT).[1] This is occurring despite the negative worldwide environmental and health consequences associated with unimaginable amounts of non-degradable[2] waste plastic accumulation[3] and the significant depletion of virgin fossil feedstocks.[1] One class of commonly used plastics for applications in which the material/product must withstand harsh mechanical and environmental conditions are engineering plastics such as polyamides. Nylon-6 was one of the first synthetic fibers discovered and developed by Schlack of IG Farben in 1938

to reproduce the properties of Nylon-6,6, which was discovered by Carothers of DuPont just three years earlier.[4] Nylon-6 is a thermoplastic polyamide produced industrially by water-assisted ring-opening polymerization (ROP) of ε-caprolactam on a 5 million tons annual scale, with the market size expected to reach \$21.5 billion in 2026.[5] It is the material of choice in many applications, such as the automotive, packaging, infrastructure, textile, and fishing gear industries, due to its physical and chemical properties, including elasticity, high tensile strength, and high chemical and abrasion resistance.[5a, 6] However, these same properties also impede biodegradation,[7] leading to persistence and accumulation in landfills and the environment.[8] For example, Nylon-based abandoned fishing nets comprise ca.10 % of ocean plastic.[9] Furthermore, Nylon production has a high carbon footprint[10] associated with significant greenhouse gas emissions.[11]

The above issues associated with Nylon illustrate the need for a circular economy in which waste plastics are recycled and repurposed.[12] Mechanical recycling, common for commodity plastics such as polyolefins or polyesters, is rarely used for polyamides since the elevated temperatures required lead to partial degradation and Nylons with inferior properties.[13] The presence of contaminants in post-consumer products further complicates pristine polymer recovery. Another traditional approach to extracting value from plastics is burning them for energy recovery.[14] However, a limitation for Nylons is that toxic HCN, CO, CO_2, and NH_3 are produced in combustion,[15] and economic value is lost since ε-caprolactam is derived from fossil feedstocks in an expensive multi-step process.[5a]

Chemical recycling[16] is an alternative approach, mainly used for polyesters[17] to recover the starting monomers, and would likewise be attractive for Nylon-6. Traditionally, ε-caprolactam is prepared from crude oil, so production by recycling Nylon-6 would alleviate pressure on finite natural resources and lower production and energy costs. Conventional Nylon-6 chemical recycling requires high temperatures (270–320 °C) and high superheated steam pressures.[18] Acids and bases such as phosphoric acid, boric acid, alkali metal carbonates, or hydroxides are also reported to accelerate depolymerization.[18,19] Sub- and supercritical alcohols,[20] as well as ammonia,[18,21] have also been employed, but additional steps are required to recover the ε-caprolactam.

In 2018, Kamimura and Yamamoto reported that Nylon-6 can be depolymerized to ε-caprolactam in 55–86 % yields in excess ionic liquids with 5–10 wt % 4-dimeth-

[*] L. Wursthorn, K. Beckett, J. O. Rothbaum, Prof. Y. Kratish, Prof. T. J. Marks
Department of Chemistry, Northwestern University
2145 Sheridan Road, Evanston, IL 60208-3113 (USA)
E-mail: yosi.kratish@northwestern.edu
t-marks@northwestern.edu

Dr. R. M. Cywar, C. Lincoln
Renewable Resources and Enabling Sciences Center, National Renewable Energy Laboratory
Golden, CO 80401 (USA)

ylaminopyridine (DMAP) as the catalyst (Figure 1A).[22] This process operates at 300 °C, with and without microwave irradiation,[22c] and ε-caprolactam was isolated after a 25-fold extraction or distillation from the ionic liquid; note that partial decomposition of the ionic liquid[22a] and DMAP occur.[22c] The high DMAP toxicity is another concern since it may contaminate the ε-caprolactam.[23] Enthaler et al. reported Nylon-6 depolymerization to N-acylated caprolactam using a DMAP catalyst in acetic anhydride[24] under microwave irradiation at 220–260 °C; N-acetylcaprolactam yields were 22–78 %.[24] This product is not the industrial Nylon-6 precursor and conversion to ε-caprolactam requires additional steps. In 2020, Milstein reported that an efficient Ru pincer amide hydrogenation catalyst also catalyzes the hydrogenative depolymerization of polyamides to amino alcohols in DMSO (Figure 1B).[25] Long reaction times (48 h), high H_2 pressures (70 bar), and an expensive, potentially toxic Ru catalyst are required. In the case of Nylon-6, the reaction products are not ε-caprolactam, and recovered monomer yields are 24–48 %.[25,26] Interestingly, for some of the other hydrogenated polyamides, the product amino alcohols can be dehydrogenated back to the corresponding poly(oligo)amides. The need for efficient catalytic chemical recycling of commercial Nylon-type materials is also highlighted by the development of new hybrid polyamides which undergo depolymerization at 290 °C/18 h in the presence of a $ZnCl_2$ catalyst.[27]

Figure 1. Approaches for the chemical recycling of Nylon-6.

Results and Discussion

Here we report that tris[bis(trimethylsilyl)amido] lanthanide complexes (**Ln^NTMS**) efficiently catalyze the depolymerization of Nylon-6 to ε-caprolactam (Figure 1C). This reaction is clean (>95 % selectivity to ε-caprolactam), provides high isolated yields (>90 %), is solventless, and to the best of our knowledge, proceeds at the lowest Nylon-6 to ε-caprolactam depolymerization temperature reported to date, 240 °C, near the Nylon-6 melting point [Eq. (1)], with catalyst loadings as low as 1 mol %. The catalytic activity scales with the lanthanide ion size, with the largest La^{3+} exhibiting the highest activity. The reaction is effective for virgin polymer and post-consumer products and is also compatible with admixed plastics such as polyethylene (PE), polypropylene (PP), and polyethylene terephthalate (PET). Kinetic investigations and DFT calculations suggest an initial deprotonation of the Nylon terminal amido N–H bond, which covalently binds the catalyst to the polymer, followed by a chain-end back-biting process in which ε-caprolactam units are sequentially extruded from the chain end (see below).

The present **La^NTMS** catalyst was recently shown to efficiently activate amide bonds in the deoxygenative reductions of amides with pinacolborane.[28] Therefore, this complex was chosen as a starting point to investigate the catalytic chemical recycling of ROP polyamides such as Nylon-6. Heating a mixture of Nylon-6 and 5 mol % of **La^NTMS** in a sealed cylindrical Schlenk flask to 240 °C for 4 h under 10^{-3} Torr of static vacuum affords near quantitative polymer conversion to ε-caprolactam in 90 % yield [Eq. (1), Table 1, entry 1]. The product readily sublimes from the reaction hot zone and deposits as crystals on the cold reactor wall [Eq. (1)]. The reaction is rapid and reaches near completion after 2 h (83 % yield, Table 1, entry 2), with only slight increases of ε-caprolactam yield upon further increasing the reaction time (3 h: 85 % yield, Table 1, entry 3). Increasing the reaction temperature to 280 °C completes the reaction within 30 min, affecting neither caprolactam yield (93 % yield, Table 1, entry 4) nor selectivity (>95 %). Replacing the static vacuum with an inert atmosphere does not significantly affect the reaction performance (83 % vs. 85 % yield, Table 1, entries 5 and 2, respectively). However, under vacuum, ε-caprolactam appears more crystalline and collects further from the reaction hot zone. Without a catalyst, only minuscule amounts of caprolactam are obtained (Table 1, entry 6), along with trace impurities assignable to ε-caprolactam cyclic oligomers,[29] which are common impurities in the industrial polymerization process.[30] These oligomers can be extracted from the Nylon-6 starting material and observed by 1H NMR in $CDCl_3$ (Figure S2).

Exchanging the –N(TMS)₂ ligands for weakly basic triflate –OTf and bistriflimide –N(Tf)₂ ligands affords poor catalytic activity (5 % and 7 % yield, Table 1, entries 7 and 8, respectively), highlighting that Lewis acidity alone cannot account for the observed activity. Furthermore, $LaCl_3$ and $La(O^iPr)_3$ exhibit negligible catalytic activity (Table 1, entries 9 and 10), demonstrating the importance of the –N(TMS)₂ ligand in the catalysis, which we attribute to the high basicity in deprotonating the more acidic amide N–H bond
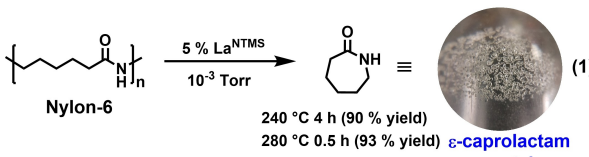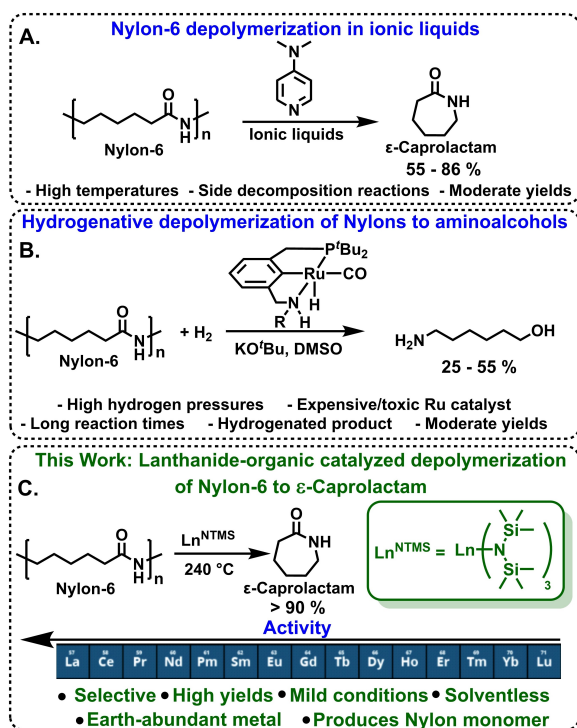
Table 1: Ligand and metal screening of Lanthanide and Group 3 catalysts in Equation (1).

240 °C 4 h (90 % yield)
280 °C 0.5 h (93 % yield)

ε-caprolactam crystals

(1)

Entry	Catalyst	Reaction time	Yield [%][a]
1	La^{NTMS}	4 h	90
2	La^{NTMS}	2 h	83
3	La^{NTMS}	3 h	85
4 [b]	La^{NTMS}	30 min	93
5 [c]	La^{NTMS}	3 h	83
6	none	3 h	1.6
7	La(NTf$_2$)$_3$	3 h	7
8	La(OTf)$_3$	3 h	5
9	La(OiPr)$_3$	3 h	1.8
10	LaCl$_3$	3 h	1.4
11	Nd^{NTMS}	2 h	61
12	Sm^{NTMS}	2 h	55
13	Gd^{NTMS}	2 h	47
14	Lu^{NTMS}	2 h	45
15	Y^{NTMS}	2 h	54
16	Sc^{NTMS}	2 h	39

Conditions: 100 mg Nylon-6, 5 mol% catalyst loading, 50 mL Schlenk flask, neat, 240 °C, static vacuum (10^{-3} Torr). [a] Yield determined by ^{1}H NMR using mesitylene as internal standard. [b] 280 °C. [c] Glovebox atmosphere (1 atm Ar/N$_2$).
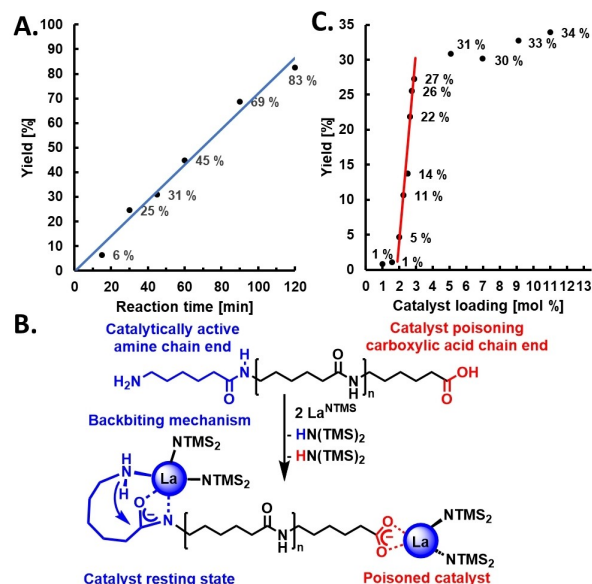
(see below). Interestingly, screening different trisamidolanthanides reveals a correlation between decreasing catalytic activity with decreasing ionic radius (Figure 2). **La^{NTMS}** (Table 1, entry 2) is the most active complex, and the activity falls in the trend, **Nd^{NTMS} > Sm^{NTMS} > Gd^{NTMS} > Lu^{NTMS}** (Table 1, entries 11–14). The caprolactam yield after 2 h at 240 °C using the smallest lanthanide ion **Lu^{NTMS}** is only 45 % (Table 1, entry 14), vs. 83 % for **La^{NTMS}** under identical conditions (Table 1, entry 2). Likewise, the catalytic activity
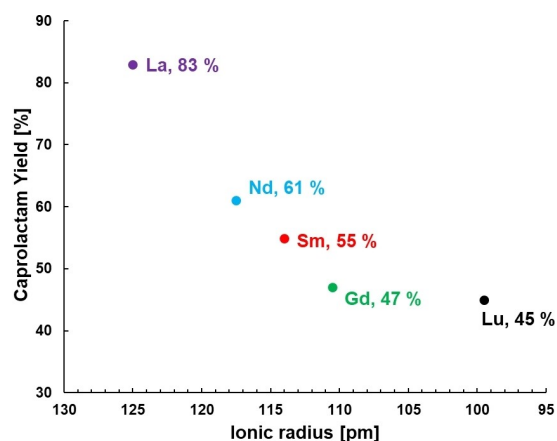
of Y and Sc, the lighter and smaller lanthanum homologs, was tested. Following the trend of decreasing catalytic activity with ionic radius, **Sc^{NTMS}** (39 % yield, Table 1, entry 16) is less active than **Y^{NTMS}** (54 % yield, Table 1, entry 15), and both are less active than **La^{NTMS}** (83 % yield, Table 1, entry 2). The lower activity for the smaller metal ions likely reflects increased non-bonded repulsions in the sterically congested transition state of the rate-determining step, where the activated amide bond, the terminal amine, and two bulky –N(TMS)$_2$ ligands are all coordinated. This is also supported by DFT calculations (see below, Figure 3).

Next, a kinetic study was carried out to better understand the catalysis on a molecular level. Since La exhibits the highest activity in this study, **La^{NTMS}** was chosen for mechanistic investigations. All the reactions were carried out under a static vacuum since this gave the highest yields and guaranteed an identical atmosphere in all reactions. Due to the lack of solvent and the viscous polymer reaction medium, classical kinetic studies in which the reaction progress is monitored in situ were not possible. Thus, a set of single-point experiments with varying reaction times and catalyst loadings was conducted to determine the rate law in substrate and catalyst concentrations.

Plotting the ε-caprolactam yield vs. time reveals a linear dependence (Figure 3A), indicating that the reaction is zero-order in Nylon-6 under the present conditions, and suggesting that in the catalyst resting state, the polyamide is bound to La center, probably after a Nylon amide (p$K_a \approx 25.5$)[32]/bis(trimethylsilyl)amine (p$K_a \approx 30$)[32] exchange. The La catalytic centers likely bind to the Nylon terminal amide moiety since, at this position, the free amine group at the

Figure 2. Yield of caprolactam for different Ln^{NTMS} catalysts vs. their ionic radii.[31] Reaction conditions, 100 mg Nylon-6, 5 % catalyst loading, 50 mL Schlenk flask, 240 °C, 2 h, static vacuum (10^{-3} Torr).

Figure 3. A) Effect of reaction time on ε-caprolactam yield. Conditions: 100 mg Nylon-6, 5 % catalyst loading, 50 mL Schlenk flask, 240 °C, static vacuum (10^{-3} Torr) B) Structure of Nylon-6 and suggested binding of the La^{NTMS} catalyst. C) Effect of catalyst loading on ε-caprolactam yield. Reaction conditions: 100 mg Nylon-6, 50 mL Schlenk flask, 240 °C, 45 min, 10^{-3} Torr. Yield determined by ^{1}H NMR using mesitylene as internal standard.

chain end can also coordinate and stabilize it (Figure 3B). This is supported by a sharp decrease in activity for acetylated Nylon-6 (See Supporting Information) and DFT calculations (see below). Gel permeation chromatographic (GPC) analysis of the residual Nylon-6 solid at different reaction times reveals a gradual fall in the average molecular mass without significant changes in the dispersity (Figure S27), supporting a backbiting mechanism[13a] in which an ε-caprolactam molecule is eliminated from the polymer-activated end in each catalytic cycle.

The dependence of the depolymerization yield on catalyst concentration reveals an interesting and informative picture (Figure 3C). From 0 to 1.5 mol% catalyst loading, no activity is observed. This initial feature can be explained by catalyst deactivation involving the reactive carboxylic acid (pK_a = 5[32]) chain ends, as shown in Figure 3B.[33] Indeed, in the case of 1 mol% **La^{NTMS}** loadings and Nylon 6 (M_n = 11930 g mol^{-1}), the calculated carboxylic acid:La ratio is ≈1:1 assuming one carboxylic acid unit per 1 polymer chain. To test this hypothesis, a Nylon-6 sample was treated with 1 M aqueous KOH solution to deprotonate the acidic chain ends. After washing and drying, catalytic depolymerization experiments were conducted with the KOH-treated Nylon-6. Rapid quantitative depolymerization is observed with only 1 mol% **La^{NTMS}** (96% isolated yield after 4 h; 94% yield after 1 h, Table 2, entries 1, 2), supporting a scenario in which the carboxylic acid groups deactivate a significant fraction of the catalytic units. Between 1.5 and 3 mol%, a steep near-linear activity increase is observed, implying the rate is essentially first order in [catalyst]. Beyond 3 mol% catalyst, the system evidences Michaelis–Menten-like saturation and even large increases in catalyst loading only marginally affect the reaction rate; in 45 min, 31% conversion for 5 mol% catalyst vs. 34% conversion for 11 mol% catalyst). Catalyst saturation would be achieved when every amide chain end was bound by a catalytic center, and another step becomes turnover-limiting. This phenomenon also supports the proposed catalyst resting state shown in Figure 3B.

Thermogravimetric analysis (TGA) experiments were next conducted on Nylon-6+catalyst mixtures to estimate the experimental activation energy. Isoconversional TGA is a standard method to investigate and extract kinetic data

from complex solid-state systems, such as the pyrolysis of polymers[19b, 34] or biomass.[35] All sample manipulations were conducted in a glovebox to maintain an inert atmosphere. The observed TGA loss can be divided into three phases: 1) 25–270°C, mass loss due to TMS$_2$N- ligand protonolysis, 2) 270–350°C, catalyzed depolymerization, 3) >350°C, Nylon-6 pyrolysis (Figures S28–S29). Four experiments at different heating rates were also conducted (Figures S28 and S30) and used to estimate the activation energies at low conversions using the Flynn-Wall-Ozawa (FWO) method (Figure S30).[36] The apparent depolymerization activation energy is E_a = 31.4 ± 3.1 kcal mol^{-1}.

Post-consumer waste plastic streams are generally composed of mixed plastics and polymer additives. To investigate the applicability of the **La^{NTMS}** catalyst to such scenarios, the depolymerization of Nylon-6 was carried out on 1:1 mixtures (by weight) with the common polymers, PE, PP, and PET. PP and PE admixture have no adverse effects on the depolymerization behavior, affording ε-caprolactam in 93% and 91% yield, respectively (Table 2, entries 3 and 4), while the unreacted PE or PP is recovered unchanged. The admixture of PET induces a slight decrease in catalytic activity, probably reflecting the presence of additional PET carboxylic acid or hydroxyl end groups (Table 2, entry 5). This process is also compatible with post-consumer Nylon-6 yarn yielding ε-caprolactam in 78% yield (Table 2, entry 6). Note that unlike the reaction with Nylon-6 powder, the reaction with Nylon-6 yarn experiences heat and mass transfer issues in the form of slow melting and minimal stirring, leading to a significant increase in the reaction time.

To further probe the Nylon-6 reaction mechanism and energetic landscape, a detailed solution-phase enthalpy profile was computed by DFT[37] for the (TMS$_2$N)$_3$La (**La^{NTMS}**)-catalyzed Nylon-6 depolymerization. First, the DFT-derived structure of **La^{NTMS}** was found to be in excellent agreement with the experimental X-ray structure,[38] validating the computational approach (Figure 4). The structure of **La^{NTMS}** possesses similar structural characteristics as previously reported lanthanide analogues,[39] however, note that this is the first time that the structure of solvent-free **La^{NTMS}** has been reported.

The secondary 6-amino-*N*-methylhexanamide was used as a Nylon-6 model for simplified computation (Figure 5A). In the first step, the amide oxygen atom is coordinated to

Table 2: KOH-treated Nylon-6 depolymerization and the effect of mixed plastics and post-consumer yarn on the catalysis.

Entry	Polymers	Catalyst loading	Reaction time	Yield [%][a]
1	KOH-treated Nylon-6	1%	4 h	97 (96)
2	KOH-treated Nylon-6	1%	1 h	94
3	1:1 mixture Nylon-6:PP	5%	6 h	93
4	1:1 mixture Nylon-6:PE	5%	6 h	91
5	1:1 mixture Nylon-6:PET	5%	6 h	77
6[b]	Post-consumer Nylon-6	4%	24 h	78%

Conditions: 100 mg untreated Nylon-6, 50 mL Schlenk flask, solventless, 240°C, static vacuum (10^{-3} Torr). [a] Yield determined by ^{1}H NMR using mesitylene as an internal standard. Isolated yield is in parentheses. [b] Inert atmosphere instead of vacuum.
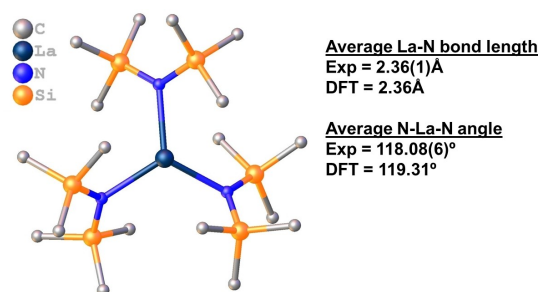

Figure 4. X-ray crystal structure of (TMS$_2$N)$_3$La (**La^{NTMS}**) (Hydrogen atoms are omitted for clarity) and experimental and calculated key bond length and angles.

Average La-N bond length
Exp = 2.36(1)Å
DFT = 2.36Å

Average N-La-N angle
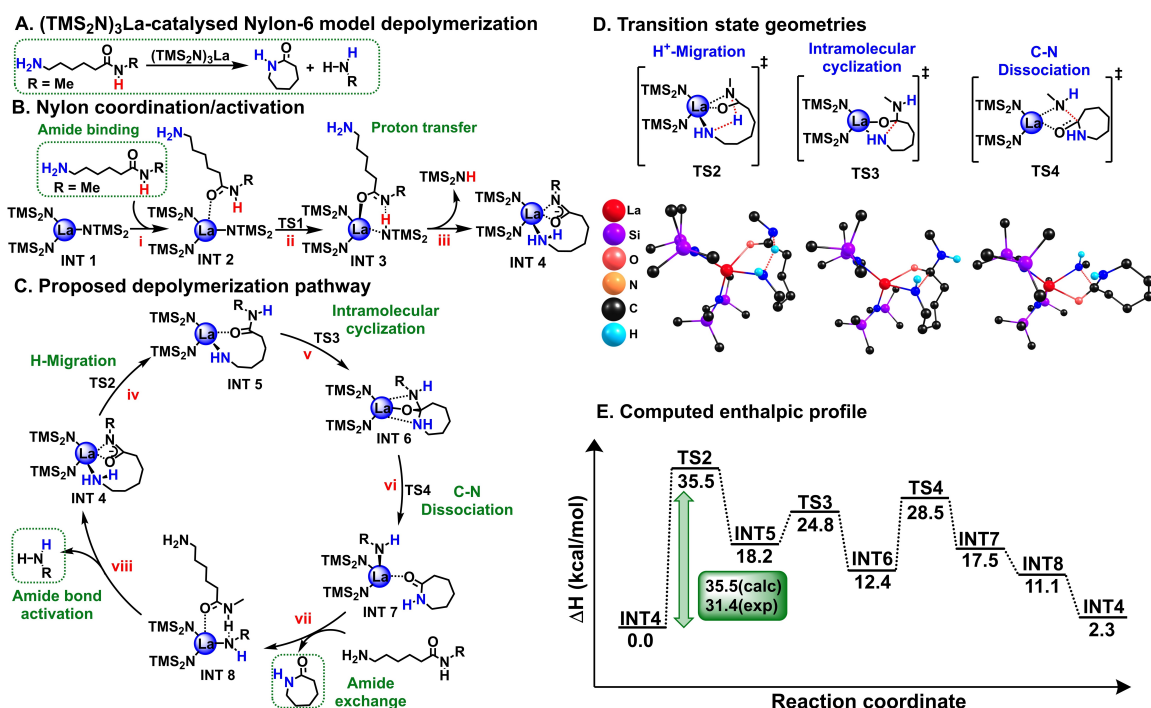Exp = 118.08(6)°
DFT = 119.31°

C
La
N
Si

Figure 5. Mechanistic DFT analysis of Nylon-6 depolymerization. A) Computed Nylon-6 model reaction. B) Nylon coordination. C) Proposed depolymerization mechanism. D) Calculated transition state geometries. E) Computed solution-phase enthalpic profile in kcal mol^{-1}.

the Lewis acidic La^{3+} in (TMS$_2$N)$_3$La (**INT1**) to produce **INT2** (Figure 5B, step i). This step is highly exothermic ($\Delta H = -20.6$ kcal mol^{-1}). Next, the amide proton migrates to the bis(silyl)amide ligand yielding **INT3**. This step is endothermic by 5.0 kcal mol^{-1} with a low energetic barrier (**TS1**) of 5.4 kcal mol^{-1} (Figure 5B, step ii). The exothermic elimination of TMS$_2$NH ($\Delta H = -2.4$ kcal mol^{-1}) yields **INT4** (Figure 5B, step iii). This step is driven by the intramolecular coordination of the primary terminal amine, which stabilizes **INT4** by 9.7 kcal mol^{-1} (Figure S31). The formation of TMS$_2$NH is also supported experimentally, where NMR indicates that 2.5 equiv of TMS$_2$NH are produced during the reaction (Figure S31). Next, **INT4** enters the catalytic cycle, and a proton transfer step from the primary amine to the amide moiety yields **INT5** in an endothermic step (18.2 kcal mol^{-1}) (Figure 5C, step iv). This step has a barrier of $\Delta H^{\ddagger} = 35.5$ kcal mol^{-1} (**TS2**, Figure 5D) and is the rate-determining transition state. Interestingly, when the primary terminal amine is replaced by a secondary amine, the barrier increases by 3.8 kcal mol^{-1} (Figure S31), highlighting once more the importance of the terminal NH$_2$ end group. Next, in an exothermic intramolecular cyclization (-5.8 kcal mol^{-1}), **INT5** is converted to **INT6** (Figure 5C, step v). The cyclization step has a relatively low barrier of $\Delta H^{\ddagger} = 24.8$ kcal mol^{-1} (**TS3**, Figure 5D). A C–N bond dissociation step in **INT6** yields **INT7**, which has the desired caprolactam product coordinated to the La center (Figure 5C, step vi). This step is exothermic by 5.1 kcal mol^{-1} and has a barrier of 28.5 kcal mol^{-1} (**TS4**, Figure 5D). Finally, caprolactam is spontaneously (-6.4 kcal mol^{-1}) released from **INT7** when another secondary amide sub-

strate coordinates to the La center yielding **INT8** (Figure 5C, step vii). Similar to steps ii and iii, amine (RNH$_2$) release from **INT8** yields starting **INT4** in an exothermic step (-8.8 kcal mol^{-1}). The overall computed reaction barrier is 35.5 kcal mol^{-1}, in good agreement with the TGA-derived $E_a = 31.4 \pm 3.1$ kcal mol^{-1}. Moreover, the calculated reaction barrier for the less active **Lu^{NTMS}** catalyst is ≈ 1 kcal mol^{-1} higher than for **La^{NTMS}** (Figure S32), in good agreement with experiment. As expected, the overall depolymerization reaction is endothermic (2.3 kcal mol^{-1}) (Figure 5E). However, the constant caprolactam sublimation from the reaction mixture shifts the equilibrium towards the products.

Conclusion

In conclusion, we demonstrate a new catalytic system based on readily accessible lanthanide trisamides that catalyze the rapid and selective depolymerization of Nylon-6 to it's industrial precursor, ε-caprolactam. The process is solvent-free, high-yielding, highly selective, and carried out under mild conditions. The catalytic activity correlates with the ionic radius of the lanthanide ion, with complexes bearing larger lanthanides demonstrating higher activities. The process is also compatible with post-consumer Nylon-6 and admixed plastics such as PP, PE, and PET. Experimental and theoretical mechanistic analyses argue that the reaction proceeds via a novel mechanism involving an initial deprotonation step of the Nylon amide N–H bond which binds the catalyst covalently to the polymer and is followed by

predominant chain-end backbiting steps in which ε-caprolactam units are sequentially excised from the chain ends.

Conflict of Interest

The authors declare no conflict of interest.

Data Availability Statement

The data that support the findings of this study are available in the Supporting Information of this article.

Keywords: Chemical Recycling · Green Chemistry · Lanthanides · Nylon · Plastic

[1] E. MacArthur, *Ellen MacArthur Foundation* **2017**, 5-60.
[2] a) B. C. Gibb, *Nat. Chem.* **2019**, *11*, 394–395; b) K. L. Law, R. Narayan, *Nat. Rev. Mater.* **2022**, 7, 104–116.
[3] a) J. R. Jambeck, R. Geyer, C. Wilcox, T. R. Siegler, M. Perryman, A. Andrady, R. Narayan, K. L. Law, *Science* **2015**, *347*, 768–771; b) A. D. Vethaak, J. Legler, *Science* **2021**, *371*, 672–674; c) D. K. Barnes, F. Galgani, R. C. Thompson, M. Barlaz, *Philos. Trans. R. Soc. London Ser. B* **2009**, *364*, 1985–1998; d) S. B. Borrelle, J. Ringma, K. L. Law, C. C. Monnahan, L. Lebreton, A. McGivern, E. Murphy, J. Jambeck, G. H. Leonard, M. A. Hilleary, M. Eriksen, H. P. Possingham, H. D. Frond, L. R. Gerber, B. Polidoro, A. Tahir, M. Bernard, N. Mallos, M. Barnes, C. M. Rochman, *Science* **2020**, *369*, 1515–1518.
[4] a) D. H. Keifer, *The Establishment of Modern Polymer Science by Wallace H. Carothers: An International Historic Chemical Landmark, Wilmington, Delaware, November 17, 2000*, American Chemical Society, Washington, **2000**; b) P. Matthies, W. F. Seydl, *History and Development of Nylon 6*, Springer Netherlands, Dordrecht, **1986**, pp. 39–53.
[5] a) B. Herzog, M. I. Kohan, S. A. Mestemacher, R. U. Pagilagan, K. Redmond, R. Sarbandi, *Ullmann's Encyclopedia of Industrial Chemistry*, Wiley, Hoboken, **2000**, pp. 1–47; b) *Polyamide-6 Market—Forecast (2022–2027)*, Furion analytics Research & Consulting LLP, Hyderabad, **2019**; c) in *Nylon—Global Market Trajectory & Analytics*, Global Industry Analysts, San Jose, **2021**.
[6] B. Deopura, R. Alagirusamy, M. Joshi, B. Gupta, *Polyesters and polyamides*, Elsevier, Amsterdam, **2008**.
[7] K. Min, J. D. Cuiffi, R. T. Mathers, *Nat. Commun.* **2020**, *11*, 727.
[8] Y. Tokiwa, B. P. Calabia, C. U. Ugwu, S. Aiba, *Int. J. Mol. Sci.* **2009**, *10*, 3722–3742.
[9] G. Macfadyen, T. Huntington, R. Cappell, *Regional Seas Reports and Studies* by UNEP, no. 185, **2009**.
[10] S. R. Nicholson, N. A. Rorrer, A. C. Carpenter, G. T. Beckham, *Joule* **2021**, *5*, 673–686.
[11] S. Bradford, R. Rupf, M. Stucki, *Sustainability* **2021**, *13*, 707.
[12] a) I. Vollmer, M. J. F. Jenks, M. C. P. Roelands, R. J. White, T. van Harmelen, P. de Wild, G. P. van der Laan, F. Meirer, J. T. F. Keurentjes, B. M. Weckhuysen, *Angew. Chem. Int. Ed.* **2020**, *59*, 15402–15423; *Angew. Chem.* **2020**, *132*, 15524–15548; b) G. W. Coates, Y. D. Y. L. Getzler, *Nat. Rev. Mater.* **2020**, *5*, 501–516; c) M. Hong, E. Y. X. Chen, *Green Chem.* **2017**, *19*, 3692–3706; d) E. Iacovidou, R. Geyer, J. Kalow, J. Palardy, J. Dunn, T. Hoellein, B. Xiong, E. Y. X. Chen, *One Earth* **2021**, *4*, 591–594; e) R. A. Sheldon, M. Norton, *Green Chem.* **2020**, *22*, 6310–6322.
[13] a) B. J. Holland, J. N. Hay, *Polym. Int.* **2000**, *49*, 943–948; b) M. J. Lozano-González, M. T. Rodriguez-Hernandez, E. A. Gonzalez-De Los Santos, J. Villalpando-Olmos, *J. Appl. Polym. Sci.* **2000**, *76*, 851–858.
[14] a) W. R. Lea, *J. Hazard. Mater.* **1996**, *47*, 295–302; b) R. Verma, K. S. Vinoda, M. Papireddy, A. N. S. Gowda, *Procedia Environ. Sci.* **2016**, *35*, 701–708.
[15] M. Nielsen, P. Jurasek, J. Hayashi, E. Furimsky, *J. Anal. Appl. Pyrolysis* **1995**, *35*, 43–51.
[16] a) A. Rahimi, J. M. García, *Nat. Chem. Rev.* **2017**, *1*, 0046; b) J. Carey, *Proc. Natl. Acad. Sci. USA* **2017**, *114*, 612–616.
[17] a) Y. Kratish, T. J. Marks, *Angew. Chem. Int. Ed.* **2022**, *61*, e202112576; *Angew. Chem.* **2022**, *134*, e202112576; b) Y. Kratish, J. Li, S. Liu, Y. Gao, T. J. Marks, *Angew. Chem. Int. Ed.* **2020**, *59*, 19857–19861; *Angew. Chem.* **2020**, *132*, 20029–20033; c) S. Westhues, J. Idel, J. Klankermayer, *Sci. Adv.* **2018**, *4*, eaat9669; d) F. Welle, *Resour. Conserv. Recycl.* **2011**, *55*, 865–875; e) V. Sinha, M. R. Patel, J. V. Patel, *J. Polym. Environ.* **2010**, *18*, 8–25; f) R. D. Allen, *Joule* **2019**, *3*, 910.
[18] C. Mihut, D. K. Captain, F. Gadala-Maria, M. D. Amiridis, *Polym. Eng. Sci.* **2001**, *41*, 1457–1470.
[19] a) K. V. Datye, *Indian J. Fibre Text. Res.* **1991**, *Mar-1991*, 46–51; b) H. Bockhorn, A. Hornung, U. Hornung, J. Weichmann, *Thermochim. Acta* **1999**, *337*, 97–110.
[20] M. Goto, M. Sasaki, T. Hirose, *J. Mater. Sci.* **2006**, *41*, 1509–1515.
[21] a) R. J. McKinney, US5302756A, **1992**; b) R. J. McKinney, US5395974A, **1994**; c) M. B. Jan, A. J. Hendrix, Y. H. Frentzen, US5668277A, **1995**.

[22] a) A. Kamimura, S. Yamamoto, *Polym. Adv. Technol.* **2008**, *19*, 1391–1395; b) S. Yamamoto, A. Kamimura, *Chem. Lett.* **2009**, *38*, 1016–1017; c) A. Kamimura, Y. Shiramatsu, T. Kawamoto, *Green Energy Environ.* **2019**, *4*, 166–170.

[23] 4-(Dimethylamino)pyridine. MSDS No. 522805. Sigma–Aldrich Inc.: St. Louis, MO. https://www.sigmaaldrich.com/US/en/sds/aldrich/522805.

[24] C. Alberti, R. Figueira, M. Hofmann, S. Koschke, S. Enthaler, *ChemistrySelect* **2019**, *4*, 12638–12642.

[25] A. Kumar, N. V. Wolff, M. Rauch, Y.-Q. Zou, G. Shmul, Y. Ben-David, G. Leitus, L. Avram, D. Milstein, *J. Am. Chem. Soc.* **2020**, *142*, 14267–14275.

[26] C. Wang, O. El-Sepelgy, *Curr. Opin. Green Sustainable Chem.* **2021**, *32*, 100547.

[27] R. M. Cywar, N. A. Rorrer, H. B. Mayes, A. K. Maurya, C. J. Tassone, G. T. Beckham, E. Y. X. Chen, *J. Am. Chem. Soc.* **2022**, *144*, 5366–5376.

[28] C. J. Barger, R. D. Dicken, V. L. Weidner, A. Motta, T. L. Lohr, T. J. Marks, *J. Am. Chem. Soc.* **2020**, *142*, 8019–8028.

[29] a) L. Peng, J. Li, S. Peng, C. Yi, F. Jiang, *R. Soc. Open Sci.* **2018**, *5*, 180957; b) D. Jenke, M. Poss, S. Sadain, J. Story, W. Smith, D. Reiber, *J. Appl. Polym. Sci.* **2005**, *95*, 1262–1274.

[30] a) H. K. Reimschuessel, *J. Polym. Sci. Macromol. Rev.* **1977**, *12*, 65–139; b) S. Kurt, J. Maier, R. Horny, S. Horn, D. Koch, J. Moosburger-Will, *J. Appl. Polym. Sci.* **2021**, *138*, 50730; c) D. Heikens, *Recl. Trav. Chim. Pays-Bas* **1956**, *75*, 1199–1204; d) G. Di Silvestro, P. Sozzani, S. Brückner, L. Malpezzi, C. Guaita, *Makromol. Chem.* **1987**, *188*, 2745–2757; e) L. Bonifaci, D. Frezzotti, G. Cavalca, E. Malaguti, G. P. Ravanetti, *J. Chromatogr. A* **1991**, *585*, 333–336; f) K. Ueda, M. Hosoda, T. Matsuda, K. Tai, *Polym. J.* **1998**, *30*, 186–191.

[31] P. D'Angelo, A. Zitolo, V. Migliorati, G. Chillemi, M. Duvail, P. Vitorge, S. Abadie, R. Spezia, *Inorg. Chem.* **2011**, *50*, 4572–4579.

[32] pKa Values Compilation (by Dave Evans and D. H. Ripin) https://organicchemistrydata.org/hansreich/resources/pka/pka data/evans pKa table.pdf.

[33] R. D. Davis, W. L. Jarrett, L. J. Mathias, *Polymer* **2001**, *42*, 2621–2626.

[34] a) I. Dubdub, M. Al-Yaari, *Polymer* **2020**, *12*, 891; b) P. Das, P. Tiwari, *Thermochim. Acta* **2017**, *654*, 191–202.

[35] a) J. Cai, D. Xu, Z. Dong, X. Yu, Y. Yang, S. W. Banks, A. V. Bridgwater, *Renewable Sustainable Energy Rev.* **2018**, *82*, 2705–2715; b) Z. Ma, D. Chen, J. Gu, B. Bao, Q. Zhang, *Energy Convers. Manage.* **2015**, *89*, 251–259.

[36] a) T. Ozawa, *Bull. Chem. Soc. Jpn.* **1965**, *38*, 1881–1886; b) J. H. Flynn, L. A. Wall, *J. Res. Natl. Bur. Stand.* **1966**, *70*, 487.

[37] Calculations were carried out using the ORCA 4.1.0 software. F. Neese, WIREs Comput Mol Sci. 2012, 2012, 2073–2078.

[38] Deposition Number 2191891 (for (TMS$_2$N)$_3$La) contains the supplementary crystallographic data for this paper. These data are provided free of charge by the joint Cambridge Crystallographic Data Centre and Fachinformationszentrum Karlsruhe Access Structures service.

[39] a) C. A. P. Goodwin, K. C. Joslin, S. J. Lockyer, A. Formanuik, G. A. Morris, F. Ortu, I. J. Vitorica-Yrezabal, D. P. Mills, *Organometallics* **2015**, *34*, 2314–2325; b) P. B. Hitchcock, A. G. Hulkes, M. F. Lappert, Z. Li, *Dalton Trans.* **2004**, 129–136; c) E. D. Brady, D. L. Clark, J. C. Gordon, P. J. Hay, D. W. Keogh, R. Poli, B. L. Scott, J. G. Watkin, *Inorg. Chem.* **2003**, *42*, 6682–6690.
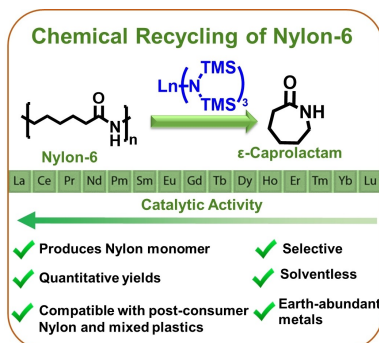
Research Articles

Depolymerization

L. Wursthorn, K. Beckett, J. O. Rothbaum,
R. M. Cywar, C. Lincoln, Y. Kratish,*
T. J. Marks* ————————— e202212543

Selective Lanthanide-Organic Catalyzed Depolymerization of Nylon-6 to ε-Caprolactam

Chemical Recycling of Nylon-6

Nylon-6 → ε-Caprolactam

Catalytic Activity

La Ce Pr Nd Pm Sm Eu Gd Tb Dy Ho Er Tm Yb Lu

✓ Produces Nylon monomer ✓ Selective
✓ Quantitative yields ✓ Solventless
✓ Compatible with post-consumer Nylon and mixed plastics ✓ Earth-abundant metals

Commercial and post-consumer Nylon-6 are selectively recycled to the ε-caprolactam monomer in high yields by readily accessible lanthanide tris(amide) catalysts in a solvent-free process. Catalytic activity scales with the lanthanide ionic radius. A chain-end backbiting mechanism is proposed from experimental and theoretical analyses.